Radiation tolerance studies of long wavelength infrared InAs/GaSb detectors

Alexander Soibel, Sir. B. Rafol, Arezou Khoshakhlagh, Jean Nguyen, Linda Hoglund, Anita Fisher, Sam. A. Keo, David Z.-Y. Ting and Sarath D. Gunapala

Infrared Photonics Group
Jet Propulsion Laboratory
California Institute of Technology

Copyright 2016. California Institute of Technology. Government sponsorship acknowledged

Outline

- Introduction
  - Barrier Infrared Detector (BIRD)
  - Complementary Barrier Infrared Detector (CBIRD)
- Proton radiation effect on CBIRD performance
  - Dark current
  - Spectral characteristics
- Summary

Copyright 2016. All rights reserved.

Introduction

Antimonides Material System for Type-II Superlattices

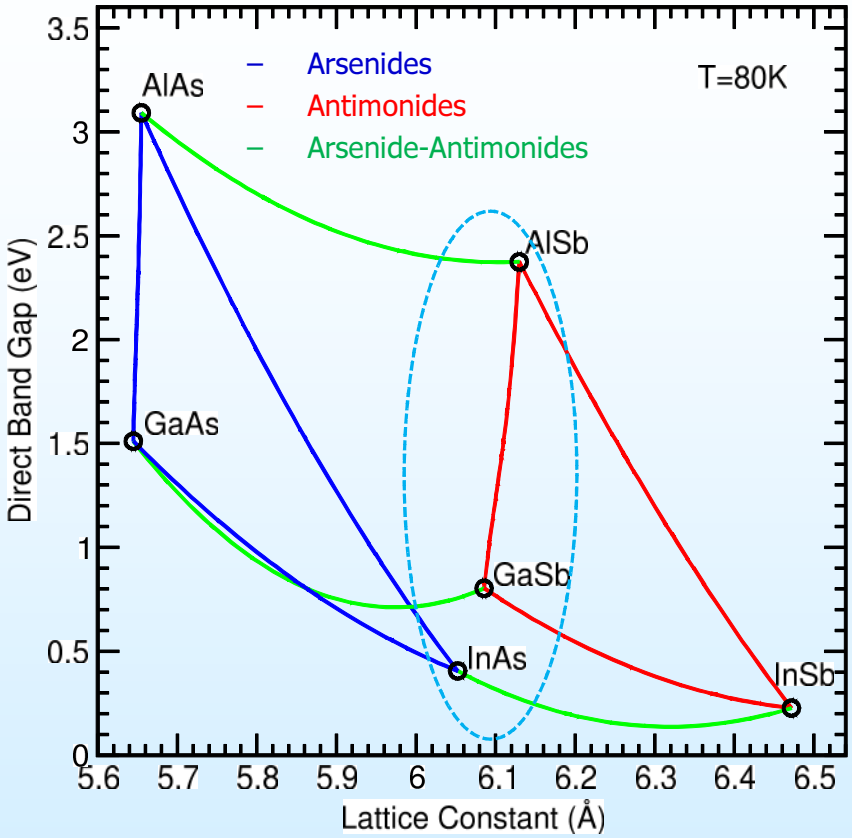

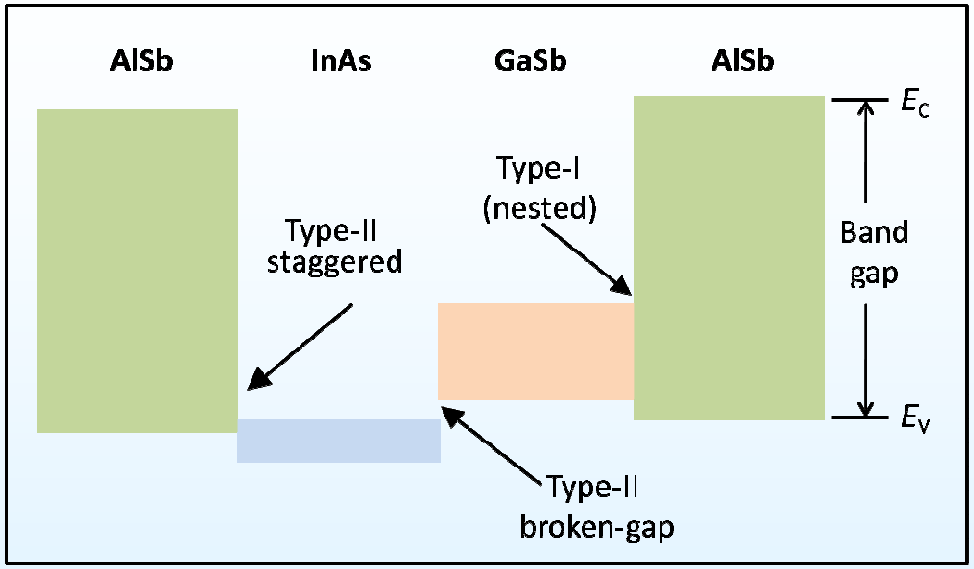

- Material system includes InAs, GaSb, AlSb and their alloys
  - Nearly lattice matched (~6.1 Å)
- Alloys with GaAs, AlAs, and InSb adds even more flexibility

- Three types of band alignments
  - Type-I (nested, straddling)
  - Type-II staggered
  - Type-II broken gap (misaligned, Type-III)
    - Unique among common semiconductor families
    - Overlap between InAs CB and GaSb VB enables interband devices
- Tremendous flexibility in artificially designed materials / device structures

Copyright 2016. All rights reserved.

Key Properties of Type-II Superlattices

- Infrared band gap
  - SWIR to VLWIR
- Absorption strength comparable to MCT

Advantages:

- Lower tunneling leakage
- Reduced diffusion dark current (p-type)
- Reduced Auger generation

Challenges:

- G-R dark current induced by SRH processes
- Lifetime significantly lower than MCT
  - Attributed to SRH
  - Effect of short lifetime on diffusion dark current ?
- Surface leakage

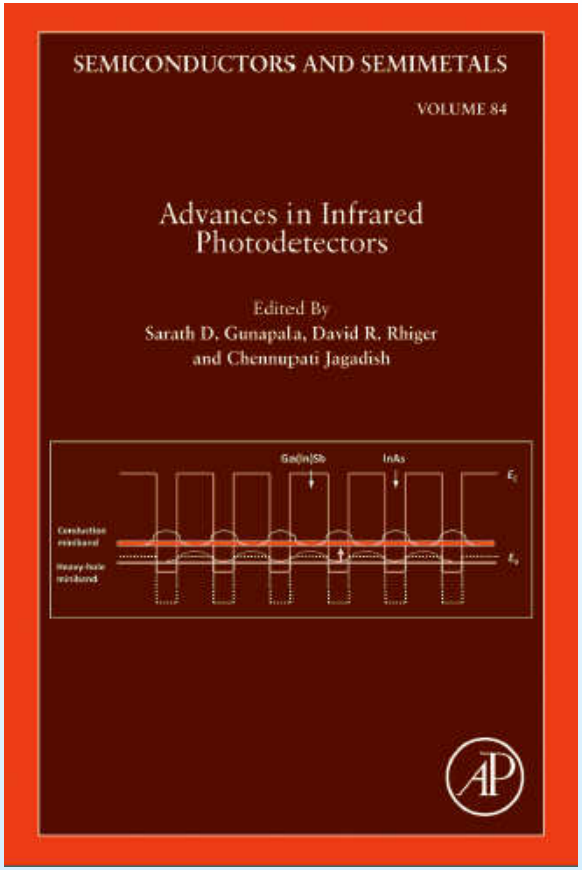

"Type-II Superlattice Infrared Detectors", *D. Z. Ting, A. Soibel, L. Höglund, J. Nguyen, C. J. Hill, A. Khoshakhlagh, and S. D. Gunapala, Semiconductors and Semimetals* **84**, pp.1-57 (2011).

Copyright 2016. All rights reserved.

G-R Dark Current Suppression using Unipolar Barriers

Barrier Infared Detector (BIRD)

- Homojunction LWIR superlattice detectors have limited performance
  - p-n, p-i-n diodes
  - Good responsivity and QE
  - High dark current

- Designs based on heterostructures can enhance performance
  - Barriers can reduce dark current
  - But do not want to cut down responsivity/QE
  - "Unipolar barriers" are particularly useful in this respect

Copyright 2016. All rights reserved.

Unipolar Barriers

Electron blocking barrier

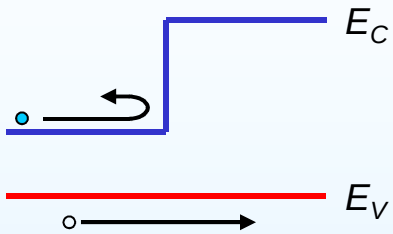

Hole blocking barrier

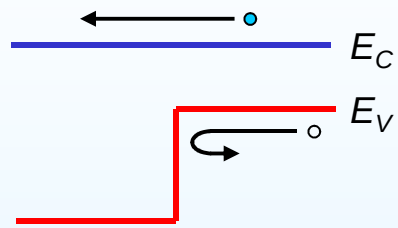

- Unipolar barriers:
  - Block one carrier type, but allows un-impeded flow of the other
  - Electron barrier
  - Hole barrier
  - Terminology introduced in Ting et al. *Appl. Phys. Lett.* **95**, 023508 (2009), now in common usage

Double Heterostructure Laser

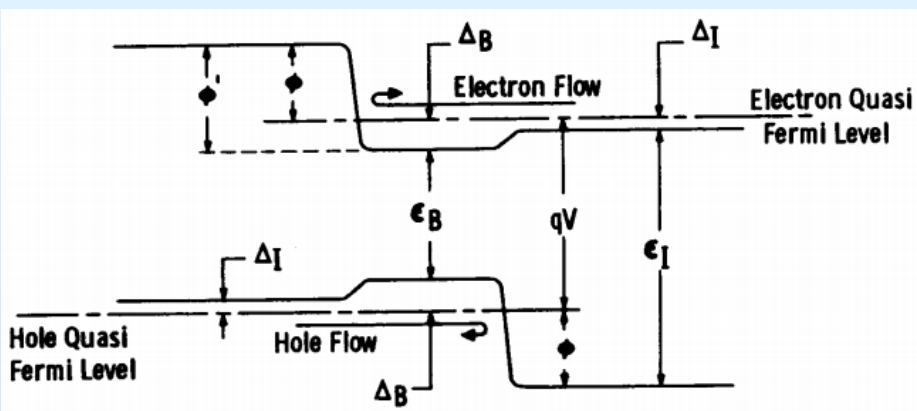

- Using unipolar barriers to enhance semiconductor device performance
  - DH Laser, H. Kroemer, Proc. IEEE 1963
  - DH Laser, Zh. I. Alferov and R. F. Kazarinov, patent certificate (Russian) 1963

Copyright 2011. All rights reserved.

SRH Suppression in LWIR SL Heterodiode

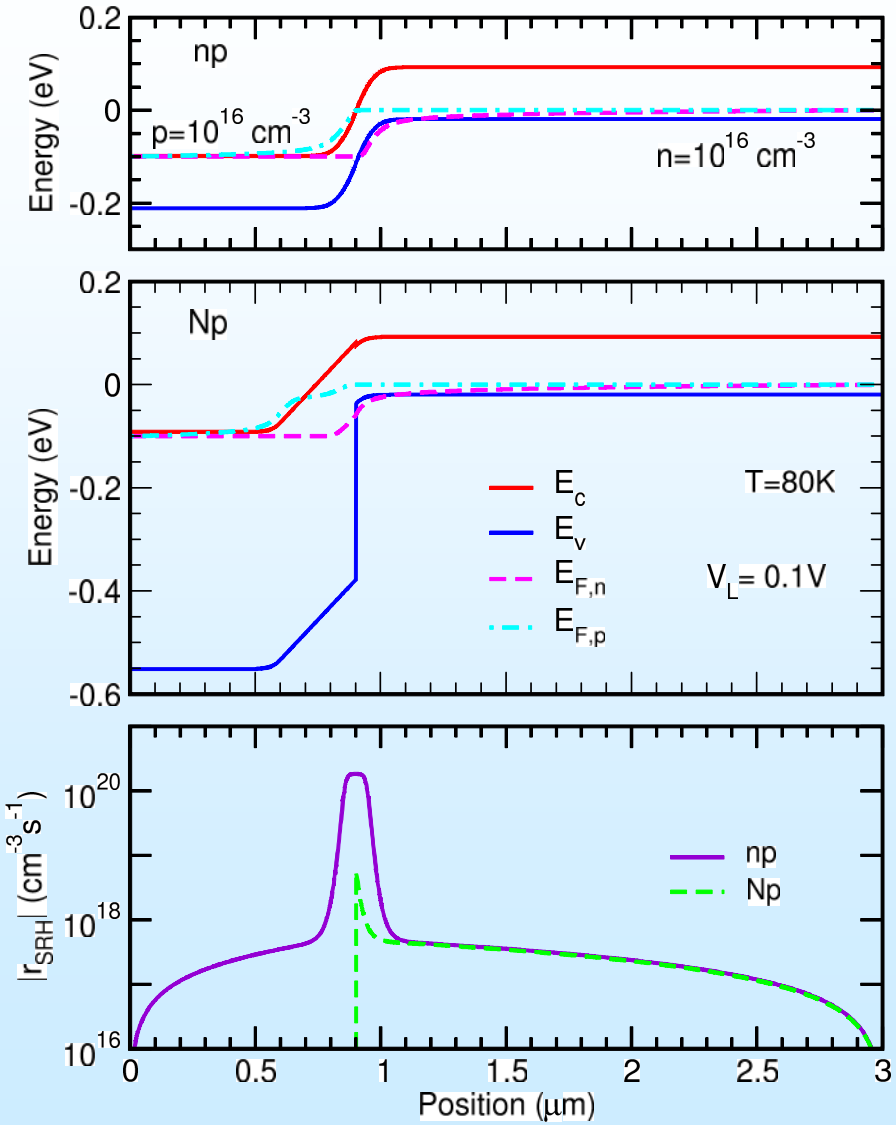

- Drift-diffusion simulation comparing LWIR SL np and Np diodes
- np homodiode
  - LWIR InAs/GaSb SL
- Np heterodiode
  - LWIR InAs/AlSb SL p-type absorber
  - InAs/AlSb SL hole-blocking unipolar barrier
  - Hole barrier does not block photocurrent
- SRH recombination rate given by

$$r_{SRH} = (np - n_i^2) / [(\tau_p (n + n_i) + (\tau_n (p + p_i)]$$

- The Np heterostructure can be effective at SRH suppression

Copyright 2016. All rights reserved.

CBIRD Structure

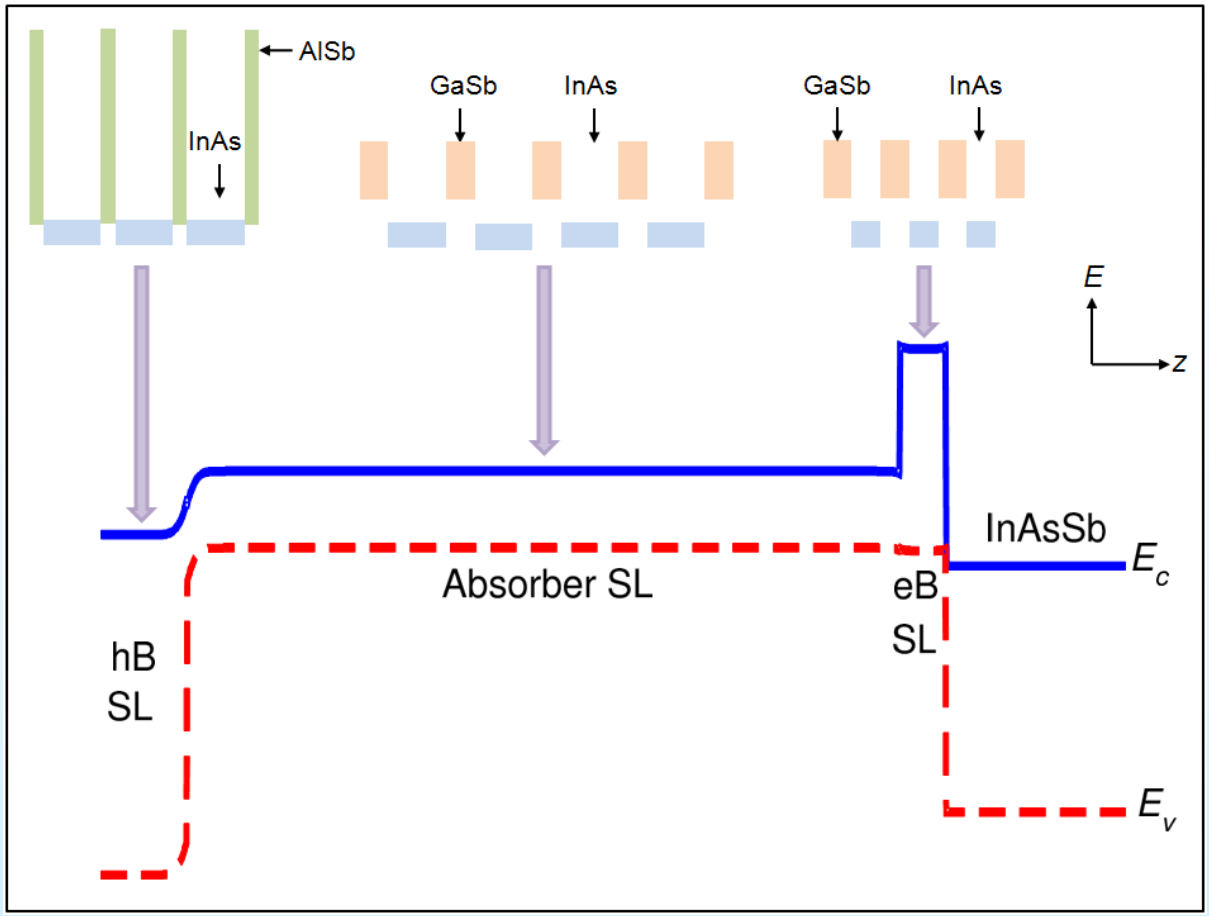

- Complementary Barrier Infrared Detector (CBIRD)
- p-type LWIR superlattice absorber surrounded by
  - n-doped unipolar hole barrier (hB)
  - p-doped unipolar electron barrier (eB)
- Bottom tunneling contact

Copyright 2016. All rights reserved.

Combination Dry Etch

Single pixel detectors were fabricated by dry etching

- $CH_4/H_2/BCl_3/Cl_2/Ar$ combination ICP dry etch technique

Detectors fully delineated

- Etching into the bottom contact

No passivation

Mounted for back-side illumination

No AR coating

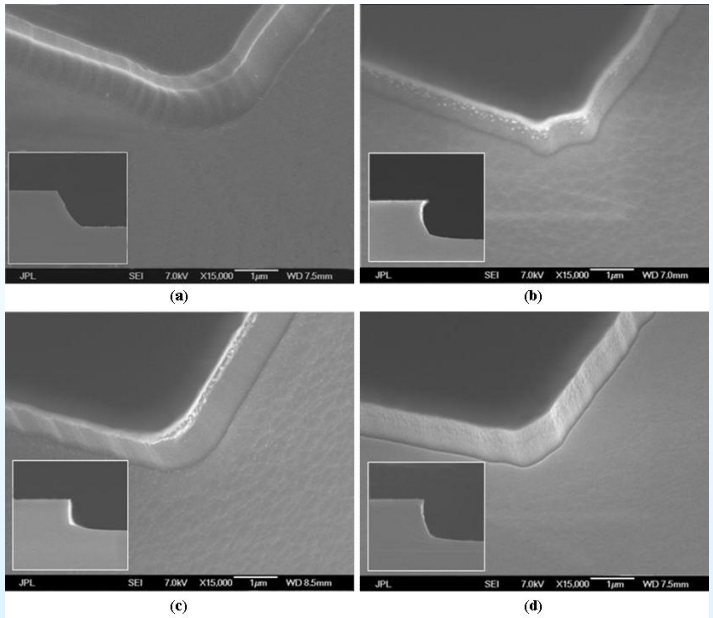

SEM images of etched detectors, from "Low dark current long-wave infrared InAs/GaSb superlattice detectors", Jean Nguyen, A. Soibel, D. Z.-Y. Ting, C. J. Hill, M. C. Lee, and S. D. Gunapala, *Appl. Phy. Lett.* **97**(5), 051108 (2010).

Copyright 2016. All rights reserved.

Device fabrication

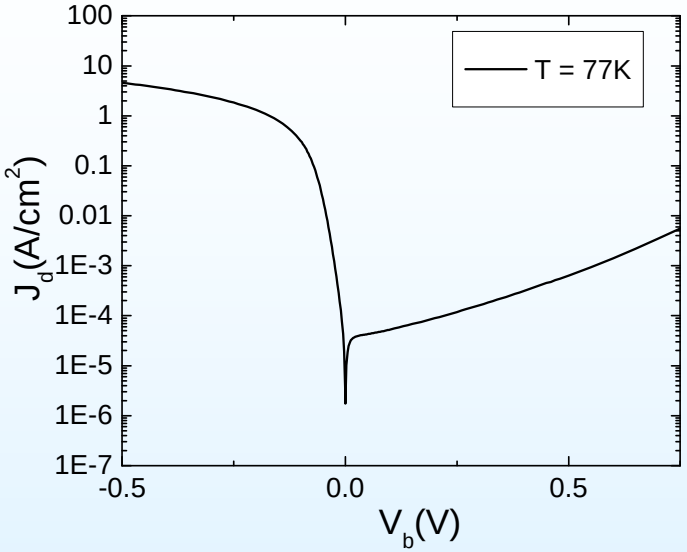

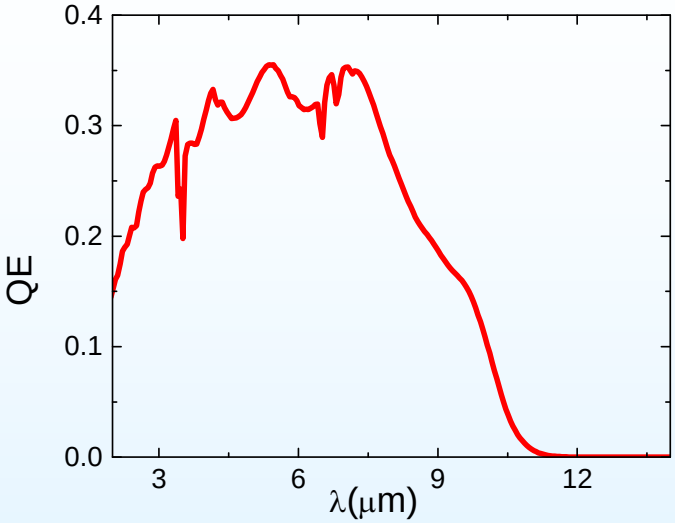

Dark current j_d = 5x10^{-5} A/cm^2 at V_b = 0.1V

Cut-off wavelength, λ_c = 10.2μm, was found from the inflection point

The maximal QE, $QE_{max} \approx 0.35$ was measured at λ = 7μm

- narrow bandpass filter centered at λ_B = 8.6μm to measure the detector photoresponse during the irradiation studies
- $QE_B \approx 0.24$ measured at λ_B = 8.6μm

Zero turn-on bias

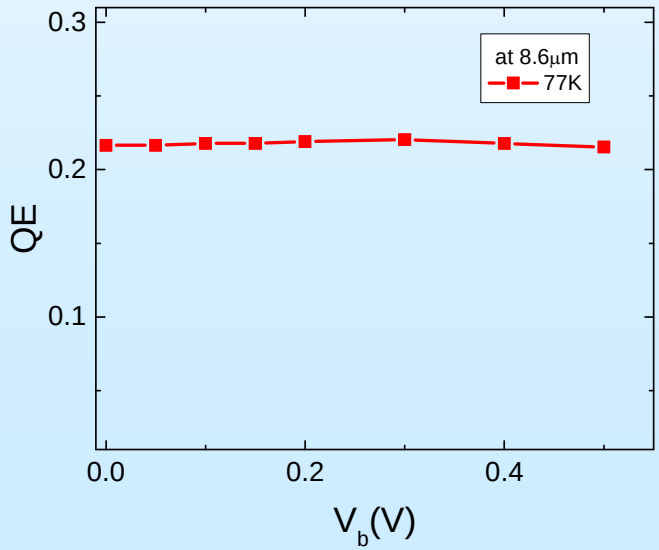

Copyright 2016. All rights reserved.

Radiation details/test

The 68MeV proton exposure was performed at cyclotron at UCD

Each radiation session was about 15min

Detectors were kept at T = 80K for duration of the study

Detectors were kept unbiased during irradiation

Dark current and photoresponse were tested prior to the irradiation and after each dose

1. Ionization damage
   - Creates *e-h* pairs
     Charge can be trapped at semiconductor-insulator interface
   - Units: Rad

2. Displacement damage
   - Results in lattice defects
   - Units: Displacement Damage Dose (DDD)
     DDD = $S \times \Phi p$,
     Φp is particle fluence
     $S = 3.3\times10^{-3}$ MeVcm^2/g for GaSb and 68 MeV protons

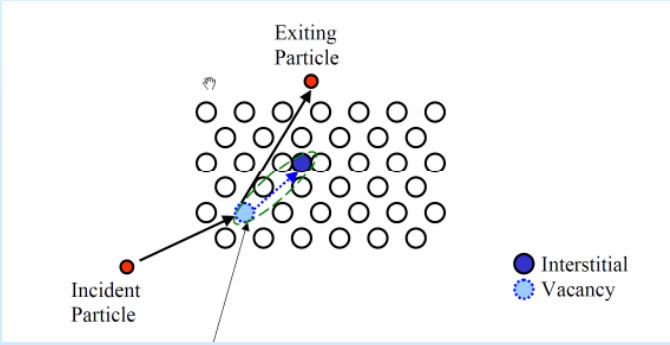

Displacement damage

Fluency [10^{11} H^+/cm^2]	Total Ionizing Dose (TID) [kRad]	Displacement damage dose (DDD) [10^9 MeV/g]
0	0	0
1.4	15	0.48
2.8	30	0.95
4.8	50	1.6
7.2	75	2.4
9.6	100	3.2
14.4	150	4.8
19.2	200	6.4

Copyright 2016. All rights reserved.

Radiation details/test

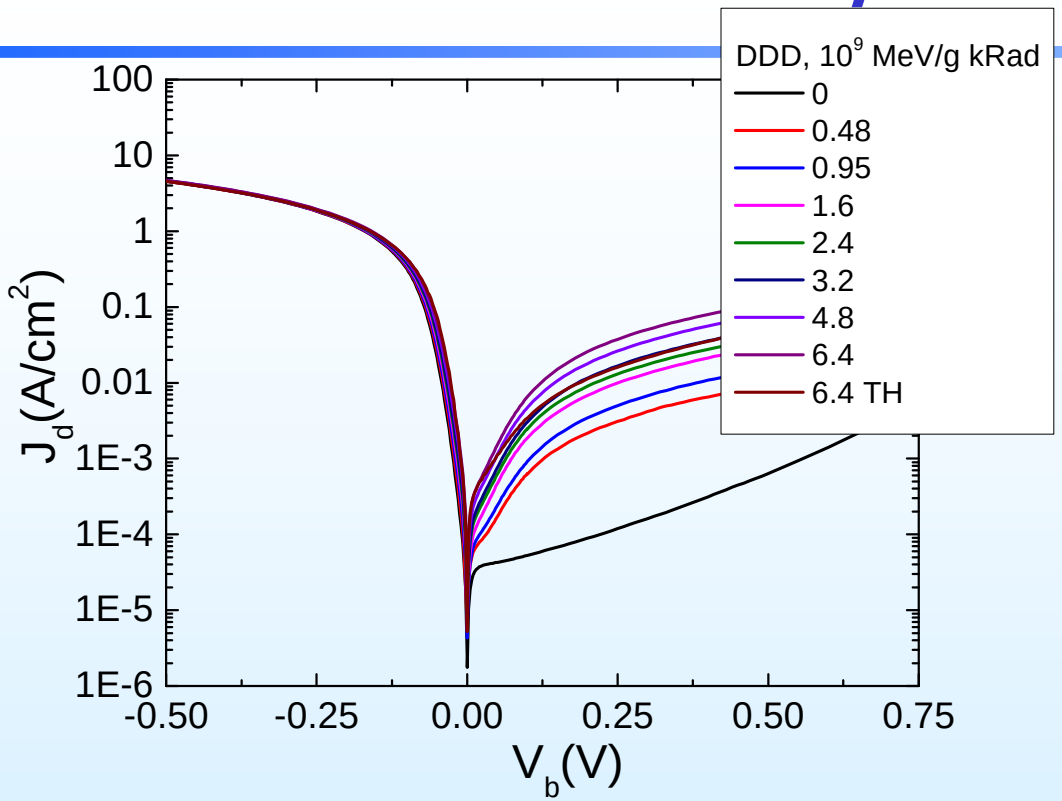

Dark current density of 150 μm square photodiode operating at T = 80 K for various DDDs.
shape of *j(V)* curves exhibits a pronounced change following the first irradiation.
Dark current density of these devices increases with DDD

$j_d = 5 \times 10^{-5}$ A/cm^2 at V_b = 0.1V at DDD = 0

$j_d = 6 \times 10^{-4}$ A/cm^2 after the first irradiation dosage with DDD = 0.48 $\times 10^9$ MeV/g

$j_d = 6 \times 10^{-3}$ A/cm^2 at DDD = 6.4 $\times 10^9$ MeV/g

Detector thermocycling ((keeping the detector at room temperature for three months) resulted only in a small reduction of dark current to jd = 4x10^{-3} A/cm^2

The radiation damage is not annealed at room temperature

Can be attributed to the displacement effects

Copyright 2016. All rights reserved.

Radiation details/test

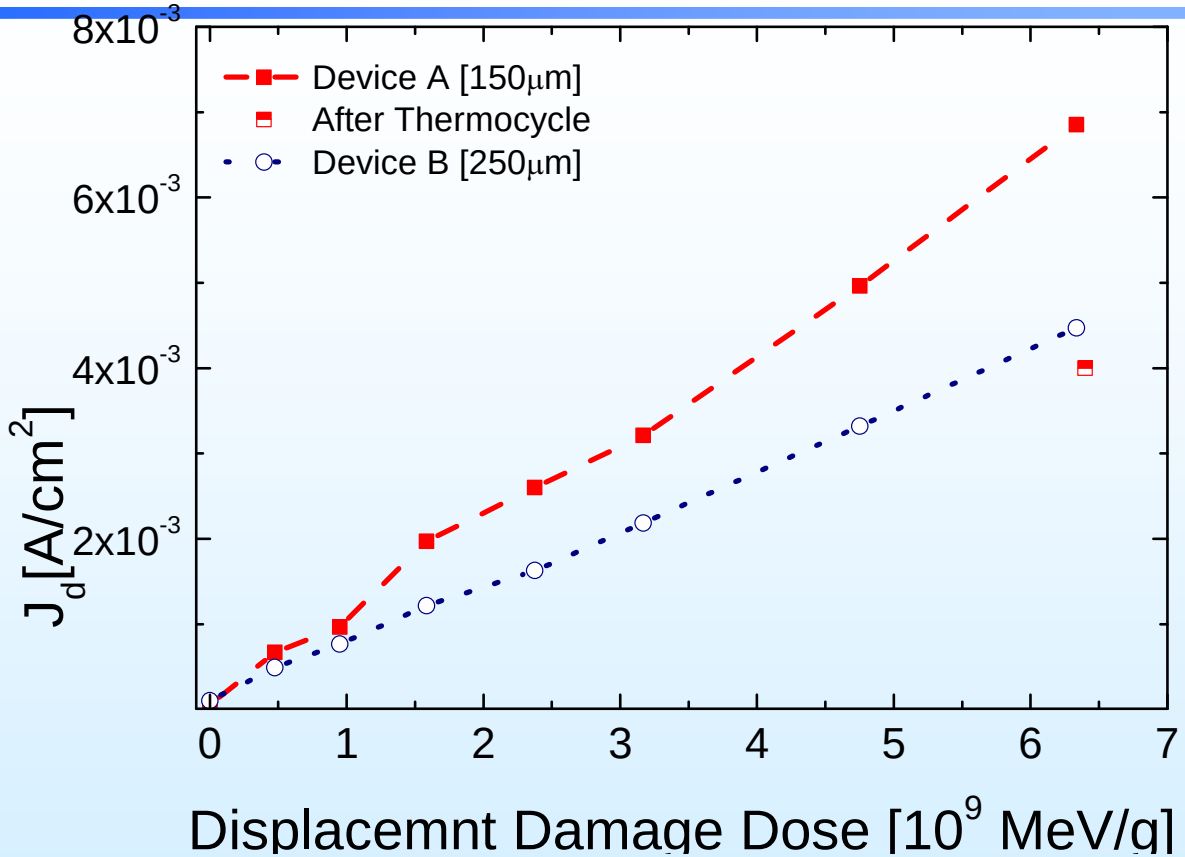

Dark current increase linearly with DDD

The change in the dark current with dose can be described, as $j_d = j_{d0} + K_{jd}\Phi p$, where

K_{jd} is the dark damage factor and

Φp is the proton irradiation fluence.

Fit to data shown in Figure 1b gives $K_{jd} \approx 2.2 - 3.5\times10^{-15}$ (A/cm^2) /(H$^+$/cm^2).

Detector thermocycling (keeping the detector at room temperature for three months) resulted in only a small reduction of dark current to $j_d = 4\times10^{-3}$ A/cm^2

This indicates that the radiation damage is not annealed at room temperature and is therefore attributed

Copyright 2016. All rights reserved.

Radiation details/test

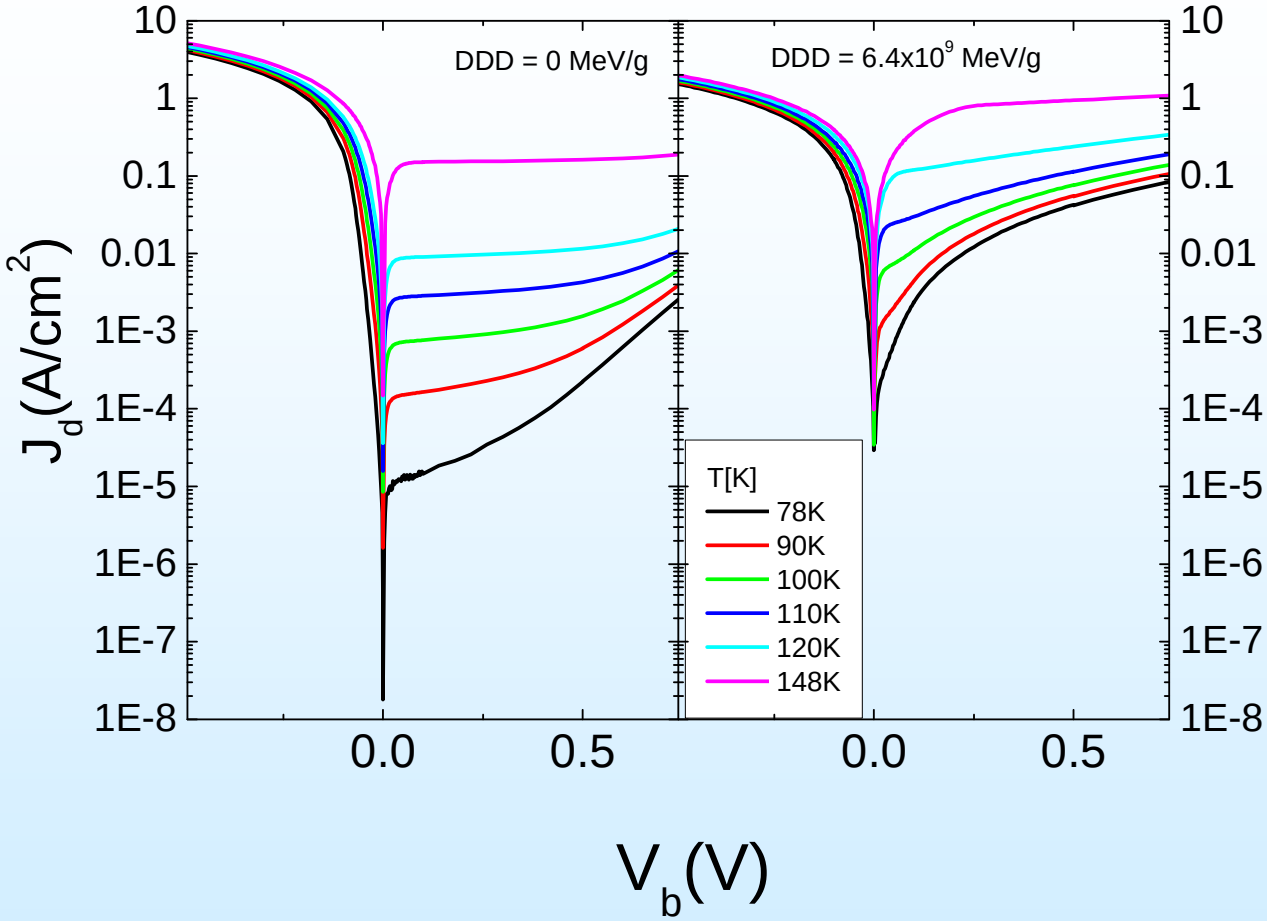

The dark current density vs. applied bias at different operating temperatures

Left: before irradiation (DDD = 0)

Right: after the last irradiation, DDD = 6.4×10^9 MeV/g

Copyright 2016. All rights reserved.

Arrhenius plot

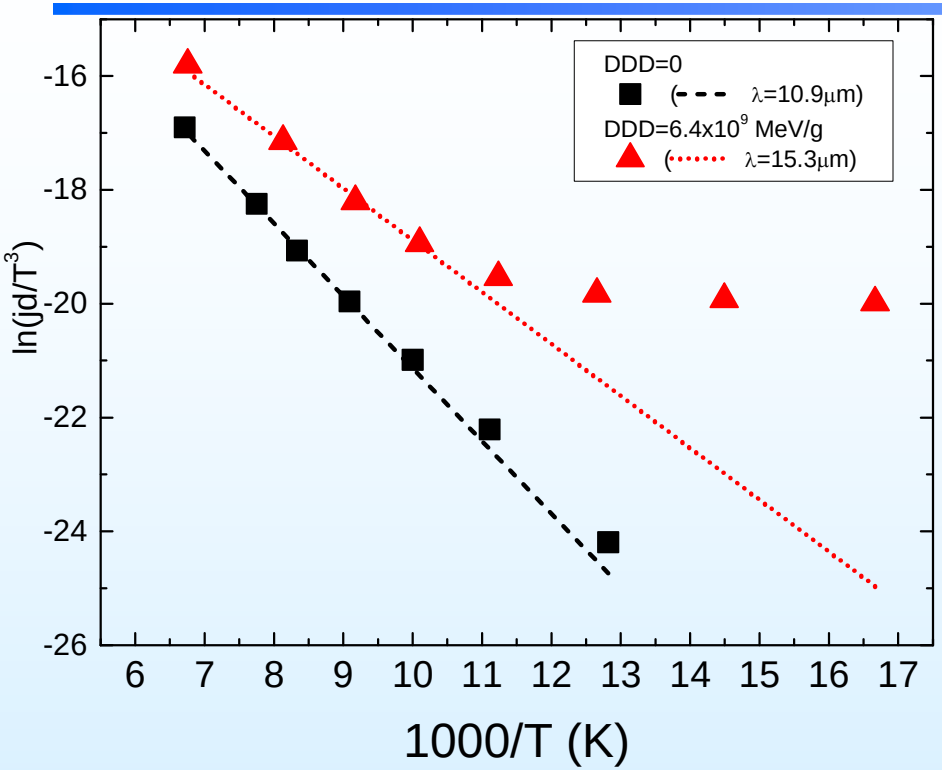

Expression for the diffusion dark current $j_{diff} \sim T^3 \exp(-Eg/k_B T)$ is used for evaluation of he temperature dependence

Before radiation (DDD = 0)

The activation energy E_{fg} = 0.115 meV derived from the data fit is very Close to the superlattice bandgap value, Eg = 0.12 meV

Diffusion dark current

After irradiation (DDD = 6.4 × 10^9 MeV/g)

The dark current becomes temperature independent at around T = 95K

Tunneling current becomes the dominant source of the dark current at lower temperature.

Moreover, the $E_{fg} \approx$ 0.080 meV in the range T = 100 - 150 K,

This is about 75% of the superlattice bandgap.

Indicates combination of the diffusion and generation-recombination processes.

Copyright 2016. All rights reserved.

Dark current mechanisms

Further understanding of the dark current mechanism changes with irradiation can be inferred from studies of the dark current dependence on the applied bias.

The three major sources of dark current in the InAs/GaSb photodioides are:

- Diffusion (j_{diff}),
- Generation-recombination ($j_{g\text{-}r}$)
- Tunneling (j_{tunn})
  at low biases mostly due to trap assisted tunneling

- The diffusion dark current: $\boldsymbol{j_{diff} = J_0\, exp(qV/k_BT)-1)}$
  J_0 is saturation current, V is applied bias, q is electron charge, and k_B is Boltzmann constant.
- Generation-recombination current : $\boldsymbol{j_{g-r} = A_{g-r}\, \frac{1}{V_{bi}-V} \sinh\left(-\frac{qV}{2k_BT}\right) \frac{\ln(\sqrt{b^2-1}+b)}{\sqrt{b^2-1}}}$;
  $b = e^{-\frac{qV}{2k_BT}}$, where $A_{g\text{-}r}$ is a constant and V_{bi} is built in potential.
- Trap assisted tunneling current: $\boldsymbol{j_{tunn} = A_{TAT} V exp\left(-\frac{B}{\sqrt{V_{bi}-V}}\right)}$
  A_{TAT} and B_{TAT} are voltage independent constants.

Copyright 2016. All rights reserved.

Jd vs V fit

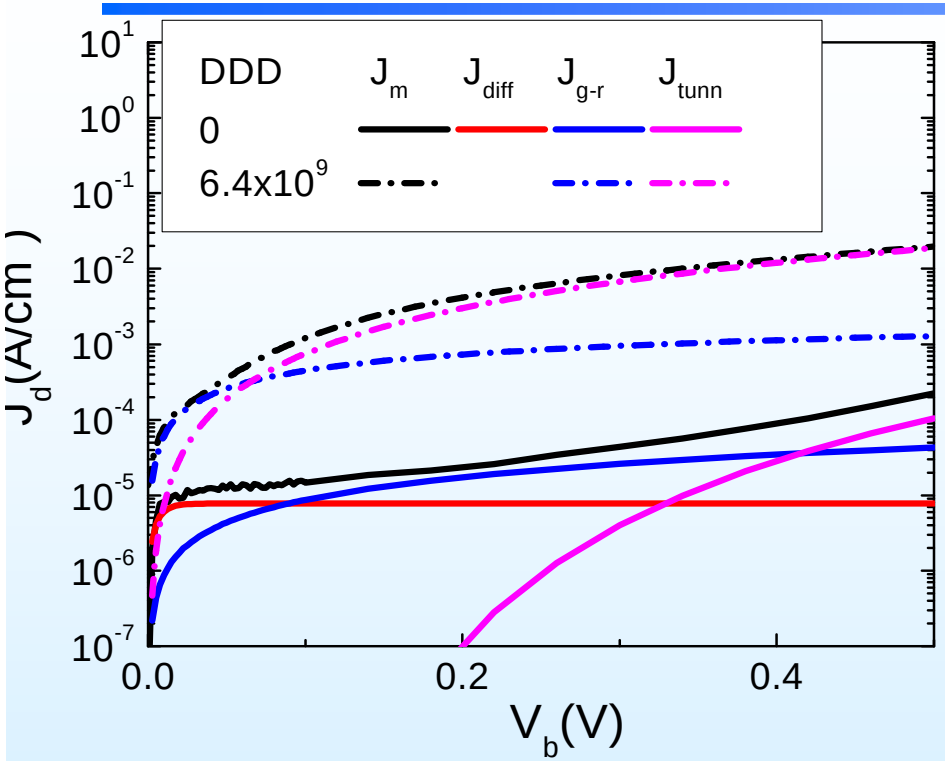

Fit of measured dark current density, j_m, at T = 80 K for DDD = 0 and 6.4 ×10^9 MeV/g with diffusion (j_{diff}), generation-recombination (j_{g-r}) and tunneling (j_{tunn}) components.

Before irradiation:

- Diffusion dark current forV_b <100mV.
- Generation-recombination current starts to dominate at higher bias and
- Tunneling current becomes the prevailing component at the applied biases above 400 mV

After irradiation with DDD = 6.4×10^9 MeV/g:

- Generation-recombination current dominates at Vb < 50 mV and
- Tunneling current starts to dominate at higher bias

These results are in good agreement with the conclusions from the J_d temperature dependence

Surface leakage current

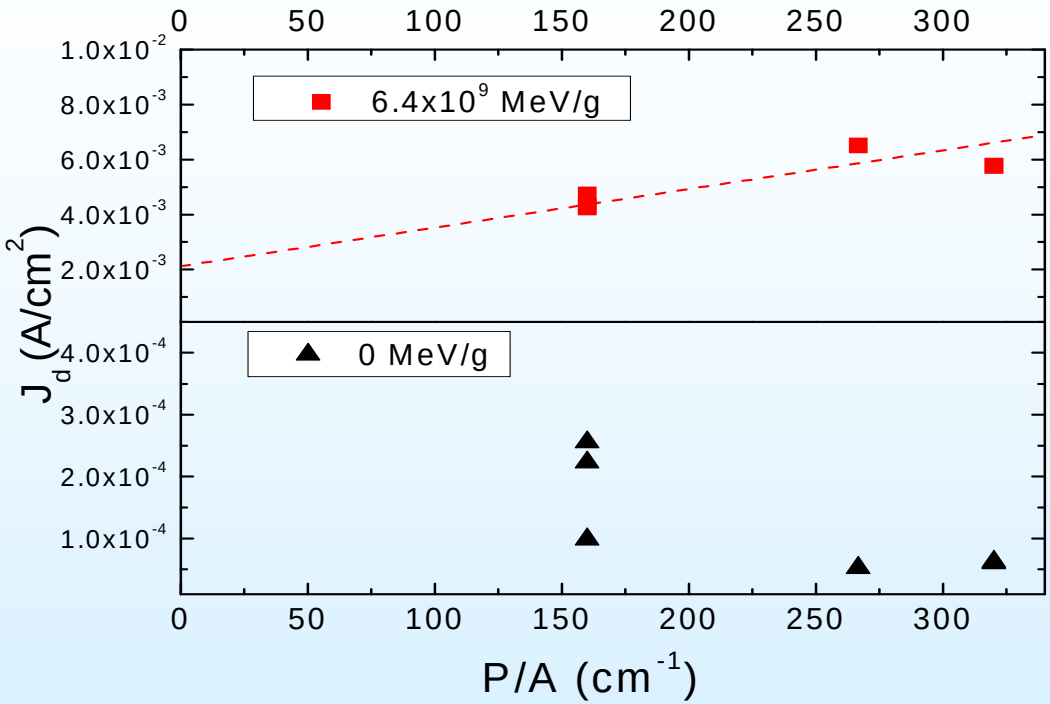

The dark current density:

$j_d = j_b + j_s \times P/A$

j_b is bulk current densities

j_s is surface current densities

Before the irradiation, there is no clear dark current dependence on the perimeter/area, P/A, ratio

After irradiation, a linear dependence of the dark current on the perimeter/area is observed

$j_{ba} \approx 2\times10^{-3}$ A/cm^2

Irradiation increases both bulk and surface dark currents, but the

Damage near the detector side wall has a larger effect on the dark current

Surface leakage observed here arises from the tunneling through defects created by the radiation near the device side walls

Copyright 2016. All rights reserved.

QE cange with radiation

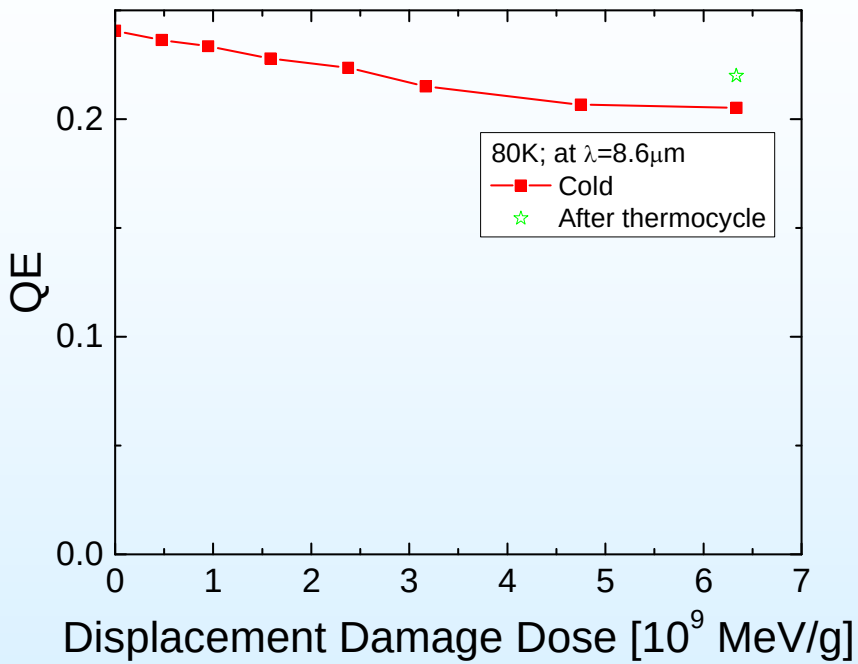

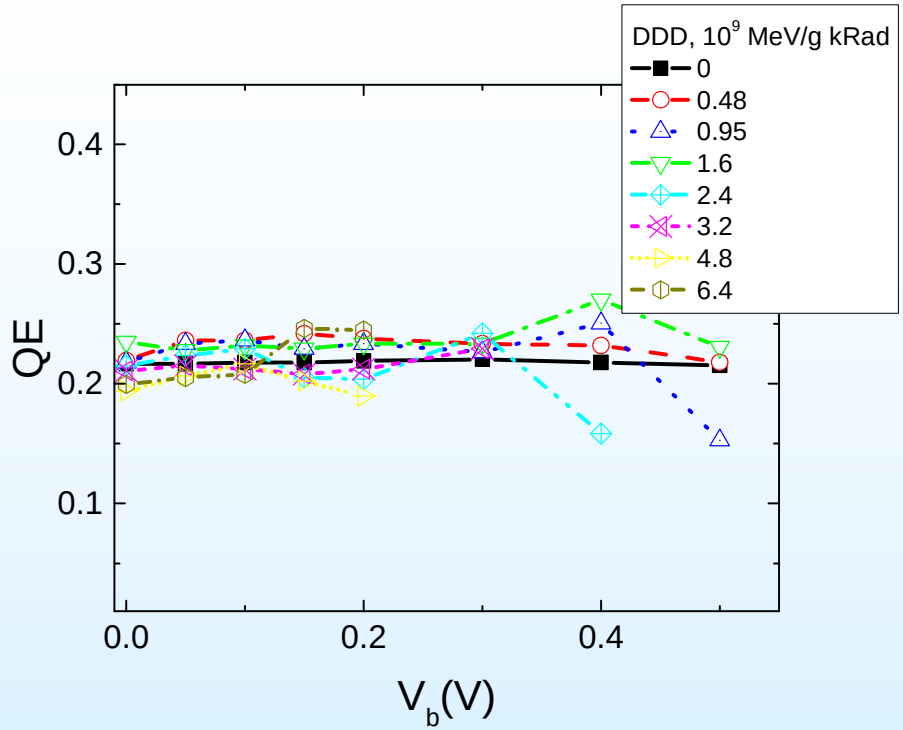

Before irradiation: $QE_B \approx 0.24$ at $\lambda = 8.6\mu m$

QE_B decreases with radiation dose

$QE_B \approx 0.21$ at DDD = 6.4×10^9 MeV/g.

15% decrease in QE over the full range of DDD.

Detector thermocycling resulted in a very minor increase of Quantum Efficiency to $QE_B \approx 0.22$

No change in turn-on bias, Von

Copyright 2016. All rights reserved.

Why only small change in QE

Two hypothesis

1. L_e >> d:

- From transmission measurements:
  Superlattice absorption coefficient (α) was estimated to $\alpha \sim 2500$ cm^{-1} at $\lambda = 7$ μm
  Substrate transmission is found to be close to 100% at this wavelength.
- Estimate the minority carriers (electrons) diffusion length, L_e, from the absorption coefficient and QE value.
  $L_e \approx$ 5-6 μm is significantly longer than the absorber thickness d = 2 μm.
- In this regime, $L_e >> d$, the decrease of the diffusion length with DDD would only result in a small degradation of QE.

2. Only a minor decrease of the lifetime with radiation?

- Minority carrier lifetime in LWIR InAs/GaSb superlattice is relatively short, $\tau \approx 30$ ns
  Due to the non-radiative recombination through defects states associated with Ga atoms and potentially assisted by multiphonon processes.
- The defects are intrinsically present in the superlattice and can continue to dominate the recombination process even after exposure to the radiation

Copyright 2016. All rights reserved.

Summary

We investigated the effect of proton irradiation on the performance of long wavelength infrared (LWIR) InAs/GaSb photodiodes (λ_c = 10.2 mm), based on the complementary barrier infrared detector (CBIRD) design

We found that irradiation with 68 MeV protons causes a significant increase in dark current from $j_d = 5\times10^{-5}$ A/cm^2 to $j_d = 6\times10^{-4}$ A/cm^2 after the first irradiation with fluence 1.4×10^{11} H^+/cm^2 and to $j_d = 6\times10^{-3}$ A/cm^2 at fluence 19.2×10^{11} H^+/cm^2.

The analysis of dark current as a function of operating temperature and bias showed that the dominant contribution changes from diffusion current to tunneling current when these detectors are irradiated. This change in the dark current mechanism can be attributed to an onset of surface leakage current.

Moreover, post-radiation thermal-cycling of the device made only minor improvement in the device performance, indicating there is proton displacement damage to the device structure.

Only small (about 15%) decrease of the Quantum Efficiency with irradiation has been observed. It was proposed that minor change in the QE with radiation may be attributed to the long electrons diffusion lengths or weak dependence of minority carrier lifetime on irradiation dose.

Copyright 2016. All rights reserved.